

## Research Article

# A Statistical Approach in Designing an RF-Based Human Crowd Density Estimation System

**S. Y. Fadhlullah and Widad Ismail**

*Auto-ID Laboratory (AIDL), School of Electrical & Electronic Engineering, Universiti Sains Malaysia, Engineering Campus, Seberang Perai Selatan, 14300 Nibong Tebal, Penang, Malaysia*

Correspondence should be addressed to Widad Ismail; [ismailwidad@gmail.com](mailto:ismailwidad@gmail.com)

Received 26 October 2015; Accepted 4 January 2016

Academic Editor: Francisco Falcone

Copyright © 2016 S. Y. Fadhlullah and W. Ismail. This is an open access article distributed under the Creative Commons Attribution License, which permits unrestricted use, distribution, and reproduction in any medium, provided the original work is properly cited.

The study of human crowd density estimation (H-CDE) using radio frequency is limited due to the nature of wireless medium and the advancement of visual-based systems. There were two statistical methods, namely, One-Way Analysis of Variance and Design of Experiment applied in designing the H-CDE system. One-Way Analysis of Variance is used to investigate the difference in signal attenuation between dynamic and static crowds. The Design of Experiment is utilized to identify significant crowd properties that affect wireless signal propagation. The significant factors were later trained into the H-CDE algorithm for the purpose of estimating the human crowd density in a defined sector. A sector comprising three placements of 2.4 GHz ZigBee wireless nodes continuously reported the received signal strength indicator to the main node. The results showed that the H-CDE system was 75.00% and 70.83% accurate in detecting the low and medium human crowd density, respectively. A signal path loss propagation model was also proposed to assist in predicting the human crowd density. The human crowd properties verified by using the statistical approach may offer a new side of understanding and estimating the human crowd density.

## 1. Introduction

Monitoring and estimating human crowd density using radio frequency (RF) is a field of largely unexplored study due to problems related to the unpredictable wireless medium, improvement of visual-based systems, and the nature of human bodies in wireless medium. Crowd density estimation (CDE) has correlation to the topic of localization due to its technical similarity.

The RF-based localization is the process of estimating the position and movement of a node within a network using various mathematical techniques and algorithms [1, 2]. The localization is able to perform location sensing [3, 4], target tracking [5], or both features at the same time [6–8]. The importance of node localization can be derived from relevant applications ranging from target tracing to safety monitoring.

Crowd control and monitoring are imperative to reduce accidents. A catalogue of crowd-related disasters during Hajj pilgrimage proves that the current systems are still insufficient to cater for the ever-increasing number of pilgrims.

The latest mishap during the Hajj pilgrimage killed more than 700 people at Mina [9], despite billions of dollars spent by the Saudi Arabia government on improving the infrastructures. This further stresses the importance of human crowd monitoring to address the issue of safety and disaster prevention.

(1) *Human Crowd Density Estimation.* Table 1 shows the previous works on RF-based H-CDE. There are two types of techniques that can be implemented in estimating a crowd size which are participatory (device-handling) and nonparticipatory (device-free). The participatory method generally depends on people counting by distributing tags (or devices) to their subjects and detecting them using portable or fixed readers. However, there is an issue of true scalability due to the requirement of dedicated involvement of participants.

Nonparticipatory is a parameter-based estimation where data such as the received signal strength indicator (RSSI) obtained between the transmitter and receiver (T-R) is analyzed. This approach is opted for in this study as it allows better scalability and easier deployment. The implementation

TABLE 1: Related works on the RF-based H-CDE systems.

Sensing feature	Related work	Platform	Highlights
Participatory	WISP-based [10]	RFID	Provides framework on crowd density, identification, and geographical data at mass event gathering
	Participatory Bluetooth [11]	Bluetooth and GPS	A system for estimating crowd density and flow at urban environment using Bluetooth on smartphones
	Augmented Stadium project [12]	Bluetooth and GPS	Provides information visualisation tool for understanding crowd activities, density, location, and speed of travel based on MANETs and wireless mesh networking
	Hand phone crowd monitoring [13]	Wi-Fi and Bluetooth	Proposed collaborative Wi-Fi and Bluetooth features inside mobile phones for density estimation
Nonparticipatory	Bluetooth collaboration [14]	Bluetooth	Proposed 6 features that estimate crowd density based on signal strength in an area of 2352.25 m <sup>2</sup>
	Electronic Frog Eye [15]	Wi-Fi	Utilizes channel state information to estimate crowd density, speed, distribution, and distance
	WSN-based [16]	TelosB WSN	Proposed a three-phase iterative process of training, monitoring, and calibrating to estimate crowd density
	Wi-counter [17]	Wi-Fi	Performs crowd counting from three phases; crowdsourcing and offline and online training
	SCPL [8]	WSN	Grid-based system that utilized high number of transmitters and receivers for crowd counting and localization

of statistical methods may also contribute to the current body of knowledge on H-CDE. The ZigBee chipset with whip antenna was selected as it fits the requirement of the design of a portable, low-powered, and low data rate system.

(2) *Human Crowd Properties on Signal Attenuation.* Understanding human crowd features such as crowd spread of people, movement, and size provides an insight into the signal fluctuation caused by bodily obstructions. The effects of human crowd distribution and velocity on the signal attenuation have been studied by Xi et al. [15] and Arai et al. [18]. However, these effects can be further investigated to better understand the signal loss caused by different crowd properties and their correlations between one another. Another signal attenuation factor of interest in the WSN deployment is the number of tags. The tags are portable nodes carried by selected agents within the crowd that may register different signal reading based on different spatial obstruction. This effect is also investigated in this study.

Crowd dynamic itself is a complex topic [19] as human beings are proven to be moving based on the projected time to potential future collision instead of using the physical distance between each other [20]. As such, removing the crowd dynamic as a factor would reduce the overall complexity of the statistical analysis, and this attempt is discussed in Section 2.1.

(3) *Design of Experiment.* Design of Experiment (DOE) is a statistical method that brings several benefits when applied to scientific problems. The benefits are listed below [21, 22]:

- (1) A DOE corrects experimental framework. It ensures that the procedure and setup of the experiment

are statistically correct before any measurement is made. For example, DOE implements randomness and repetition which addresses the issue of biasness.

- (2) The DOE validates the findings of the proposed model and the results. It can be used as a validation mechanism when the proposed solution has no equivalent comparison in the literature or from modelling simulation.
- (3) It allows the verification of all interactions between parameters involved and the degree of their significance. This solves the problem of “one-factor-at-a-time experiments” which is the incomplete conclusion that resulted from the effect of a single parameter measured one at a time.

The objective of this paper is to identify and discuss the significant factors affecting the signal propagation in human crowded vicinity by using statistical methods which are the DOE and One-Way Analysis of Variance (ANOVA). Once the effect of human crowd is understood, the information is integrated into the H-CDE system for classification and modelling.

## 2. Design and Experimental Framework

*2.1. One-Way Analysis of Variance: Eliminating Human Crowd Dynamics.* The aim of this step is to remove human crowd movement as a factor in the DOE test studied in Section 2.2 so that the complexity of this study can be reduced. This is done by using One-Way ANOVA to determine whether the static and dynamic crowds (human walking speed) possess similar

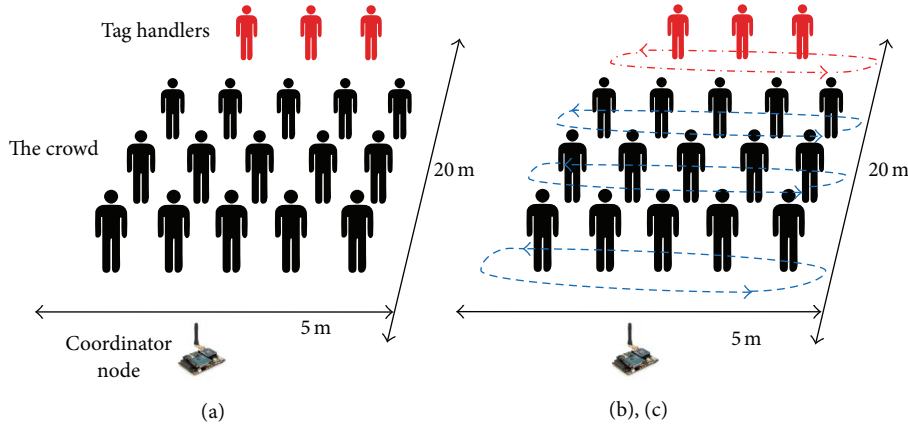


FIGURE 1: The experimental setup where (a) all elements are static, (b) only the human crowd is moving to and fro within the stipulated area, and (c) both the tag agents and human crowd are moving.

statistical effects on the signal attenuation. The hypotheses are given as

$$\begin{aligned}
 H_0: \mu_S &= \mu_{DTS} = \mu_{DTD}, \\
 H_1: \mu_S &\neq \mu_{DTS} \neq \mu_{DTD},
 \end{aligned} \tag{1}$$

where  $H_0$  and  $H_1$  are the null and alternate hypothesis, respectively,  $\mu_S$  is the mean for static human crowd and tags,  $\mu_{DTS}$  is the mean for dynamic human crowd and static tags, and  $\mu_{DTD}$  is the mean for dynamic human crowd and tags.

Figure 1 shows the layout of the experiment where the people and tag handlers stay immobile or move to and fro within the boundaries set. The walking speed was assumed to be around 1.2 m/s [18]. The mechanism for collecting the RSSI from the tags would be similar to the one in the DOE experiment, which will be later explained in Section 2.3.1. The analysis was conducted by using Minitab 16.2.3 software with 5% Tukey's family error rate.

**2.2. Design of Experiment: Identifying Significant Factors.** The objective of the DOE test is to identify the crowd properties that have significant effects on the signal attenuation. These effects would influence the H-CDE system and algorithm in Sections 2.3 and 2.4, respectively. The list of factors and their respective levels are tabulated in Table 2 while the arrangement of the DOE is illustrated in Figure 2. The number of people in a crowd is including the tag handlers while the crowd pattern is based on the people crowd density in an area of  $1 \text{ m}^2$  test. The DOE full factorial template was generated by using Minitab software with two repetitions for a total of 108 experiments and 1080 measurements.

### 2.3. System Setup for Real-Time Experimentation

**2.3.1. Developed Design of Experiment.** The coordinator's Application Program Interface (API) collected the RSSI information by using specified ZigBee command programed

TABLE 2: Factors and levels of the DOE test.

Factors	Level 1	Level 2	Level 3
Crowd size (people)	5	10	15
Crowd pattern	Scattered	Lumped	—
Crowd location (m)	10	20	30
Number of tags	1	2	3

at the microcontroller. The command issued to each tag and router triggered the nodes to reply with the RSSI of the last hop. The RSSI from tags 1, 2, and 3 and router 1 were collected sequentially with a time delay of 4 s between each sequence to allow for any retransmission to be completed. The average RSSI was calculated from 5 measurements collected from each transmission session. The RSSI from router 1 was used to train the H-CDE system and algorithm in Sections 2.3.2 and 2.4, respectively.

The block diagram of the prototype tag is shown in Figure 3. Each of the H-CDE tags is powered by a 1 W solar cell with a 2000 mAh lithium ion polymer battery as the storage element. The energy harvesting capability and Secure Digital (SD) card-based data logger are available on the tag which are features that have been used in a previous work [23].

The coordinator and router 1 nodes are made of Arduino and breakout boards connected to laptops. The transmission circuits were set to the maximum power level of 4 with enabled boost mode while the rest was kept on default settings. The RSSI data collected by the coordinator was then forwarded to the H-CDE algorithm for human crowd classification. The tags were attached to the chest of the human body; in a similar way a name tag is worn. The tags were approximately 1.24, 1.33, and 1.40 m above the ground while the coordinator and router 1 were placed 1 m above the ground.

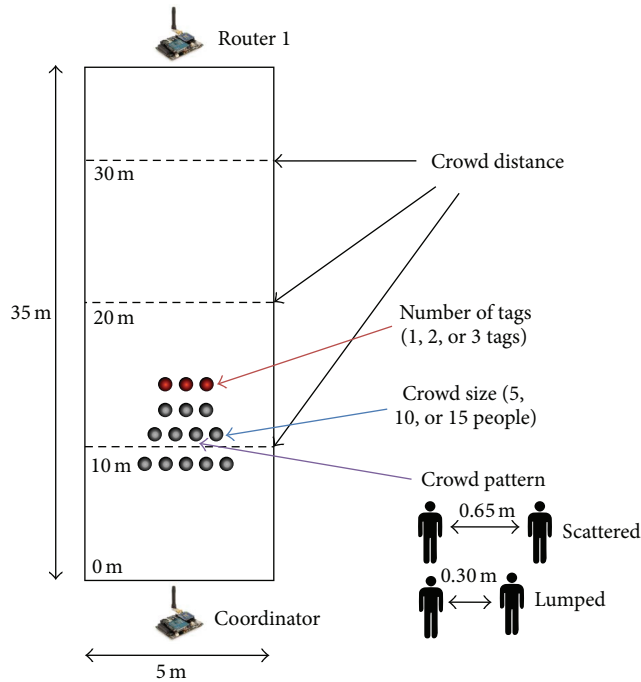


FIGURE 2: Experimental setup of the DOE. The crowd distance is measured from the coordinator while the tag agents are always placed behind the main crowd.

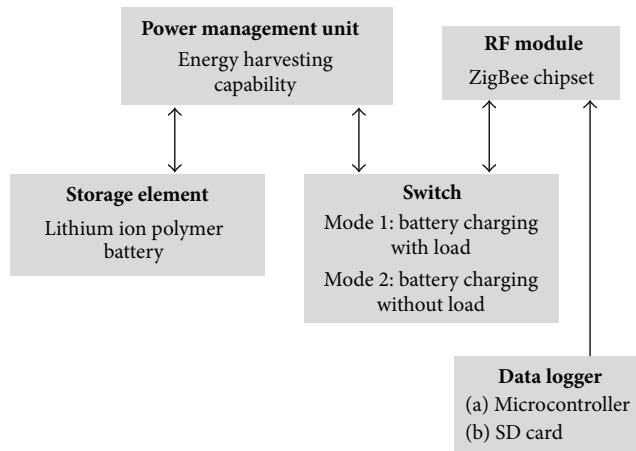


FIGURE 3: The block diagram of the H-CDE tags.

**2.3.2. Human Crowd Density Estimation System.** A moving node presents a challenging problem for the H-CDE as the node may shift its position arbitrarily in any direction in the future, rendering the instantaneous estimation largely inaccurate. A practical solution to this problem is to fix the behaviour of the tag by setting a predetermined path of its movement or by assigning the tag as a static anchor. The latter approach is implemented in the H-CDE system.

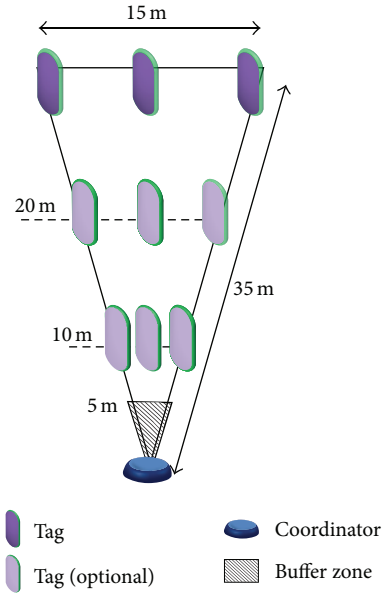


FIGURE 4: Proposed tags arrangement for the H-CDE system.

The H-CDE system utilizes three tags anchored within a defined sector as shown in Figure 4. For a complete coverage of the Mataf, 15 sectors are required. The optional tags could be placed to enhance the human crowd density estimation and localization. However, they can cause disruptions to the crowd flow and safety, and thus they are not implemented in this study. The tags are placed 35 m away from the coordinator and the RSSI of the three tags are collected continuously within 1.5 s for every 5 s. The buffer zone is a crowd-free zone that represents the half cross section of the Kaabah.

### 2.3.3. The Scope and Limitations of the Human Crowd Density Research

- (1) Modelling an individual body attenuation factor was not pursued as it is assumed that different body parts and body size absorb almost the same amount of energy [15, 17, 18]. The average height and mass of the people forming the crowd are 163.20 cm and 66.28 kg, respectively, and they are pure Asian.
- (2) The Mataf, the circumambulation and open-air area around Kaabah in Makkah (Mecca) for the Tawaf ritual during Hajj pilgrimage, is a popular target for extreme CDE using simulations [24, 25]. The coverage area of this study was based on a portion of the internal ground level of the New Mataf Extension Project, which covered an area of 70 m diameter.
- (3) The experiments were conducted outdoors to minimize the RF interference, avoid the complex multipath propagation experienced indoors, and allow the operation of the energy harvesting feature on the tags.
- (4) The size of the crowd was limited to 15 people based on the sensitivity level of the RF module used and

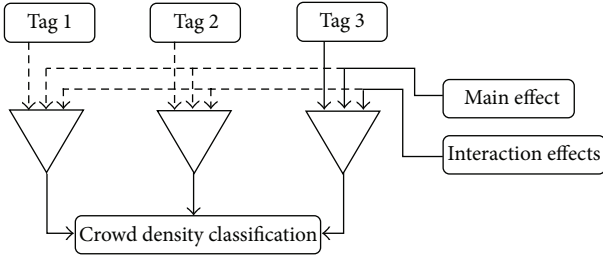


FIGURE 5: Block diagram of the H-CDE algorithm.

the “always connected” requirement of the statistical analysis.

- (5) Although guidelines had been given to the participants of the experiments, the freedom of natural human traits such as slight free movements, approximation of proximity, and comfortable standing stance were allowed to imitate the actual human behaviours.
- (6) Multihop feature was disabled.

**2.4. Human Crowd Density Estimation Algorithm.** The H-CDE algorithm fed the RSSI data obtained from three tags which were then compared with the DOE main and interaction effects produced from Section 2.2. The concept of the algorithm is shown in Figure 5. The average RSSI was calculated based on the recorded information of all tags and classified into three crowd density categories which are low, medium, and high.

The crowd density classification is given as follows:

Low density (LD):

$$LD \leq \text{RSSI}_{\text{ave}_5} + \text{RSSI}_{\text{crowd\_pattern}}$$

Medium density (MD):

$$\text{RSSI}_{\text{ave}_5} + \text{RSSI}_{\text{crowd\_pattern}} < MD \leq \text{RSSI}_{\text{max}_{15}} + \text{RSSI}_{\text{crowd\_pattern}}$$

High density (HD):

$$HD > \text{RSSI}_{\text{max}_{15}} + \text{RSSI}_{\text{crowd\_pattern}}$$

where  $\text{RSSI}_{\text{ave}_5}$  is the average signal attenuation of a crowd consisting of 5 people,  $\text{RSSI}_{\text{crowd\_pattern}}$  is the average signal difference between scattered and lumped crowd of the crowd pattern \* number of tag interactions, and  $\text{RSSI}_{\text{max}_{15}}$  is the maximum signal attenuation of the 15 people’s crowd.

In addition, the signal path loss propagation model is a useful method for supplementary crowd prediction. The empirical model is given as

$$PL = PL_0 - 10n \log_{10}(d) - X, \quad (2)$$

where  $PL_0$  is the RSSI at 1m T-R separation,  $n$  is the path loss exponent,  $d$  is the T-R distance, and  $X$  is the shadowing effect caused by the crowd. However, empirical modelling is

TABLE 3: One-Way ANOVA results from Minitab where the bolded terms highlight the most relevant information of  $p$ ,  $S$ , and  $R$ -squared values.

Source	DF	SS	MS	$F$	$p$
Factor	2	68.8	34.4	0.54	<b>0.596</b>
Error	12	762.8	63.6		
Total	14	831.6			

**S = 7.973, R-Sq = 8.27%, R-Sq (adj) = 0.00%**

often less accurate but offers simpler estimation. Prediction accuracy can be improved using deterministic methods such as the 2D ray launching [26] or full-wave simulations albeit at an increased complexity.

### 3. Results and Discussion

**3.1. One-Way Analysis of Variance.** Table 3 shows three important pieces of information which are the  $p$  value ( $p$ ), standard deviation ( $S$ ), and  $R$ -squared ( $R$ -Sq). As the  $p$  value of 0.596 is greater than  $\alpha$  (0.05), thus the null hypothesis is not rejected since the differences between the means are not significantly different. The standard deviation is mediocly high at 7.973 dBm due to the unpredictable and fluctuating signal attenuation caused by the human crowd. The value of  $R$ -squared at 8.27% is extremely low indicating that the effect of crowd on signal attenuation cannot be estimated from a specific equation formed by the Minitab software. This assumption is considered true based on the usage of three tags instead of one that contribute to different sets of the RSSI, thus making a single equation-fitting unfeasible.

The close values of mean shown in Figure 6 strengthen the assumption that the mean of the three cases is statistically nondifferent. DTD has the lowest mean as the signals from the tags could propagate better between people as a result of the posture and extraspatial requirement of a moving person.  $S$  has the highest mean as the signals from the nodes are relatively less fluctuated due to the fixed positions of the tags and human crowd.

As a summary from Table 3 and Figure 6, the signal attenuation caused by the effect of moving and stationary tags and human crowd is statistically the same. Thus, the influences of the mobile tag and human crowd can be removed as the factors in the DOE test, therefore effectively reducing the number of factors from seven to four.

**3.2. Design of Experiment Analysis.** Figure 7 shows three sources which have significant effects on the signal attenuation. The effects are denoted by having  $p$  value less than or equal to  $\alpha$  (0.05). The main effect is the human crowd size ( $A$ ), and the interaction effects are crowd size \* number of tags ( $A * D$ ) and crowd pattern \* number of tags ( $B * D$ ). Figure 8 shows the second iteration of the same analysis which only involves the influences of significant main and interaction effects. This step further strengthens in verifying that only three factors inflict significant effects on signal attenuation.

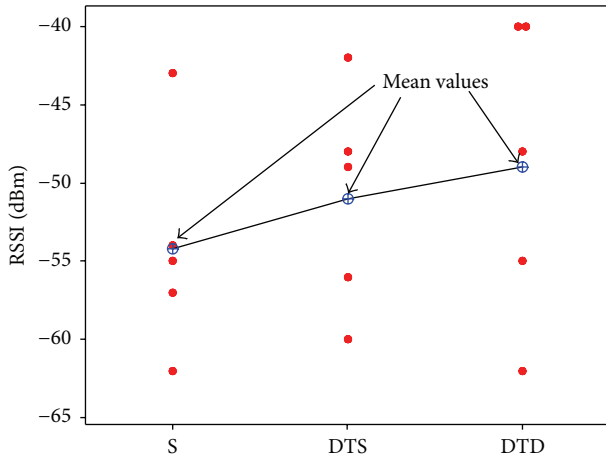


FIGURE 6: Individual value plot of static human crowd and tags (S), dynamic human crowd and static tags (DTS), and dynamic human crowd and tags (DTD).

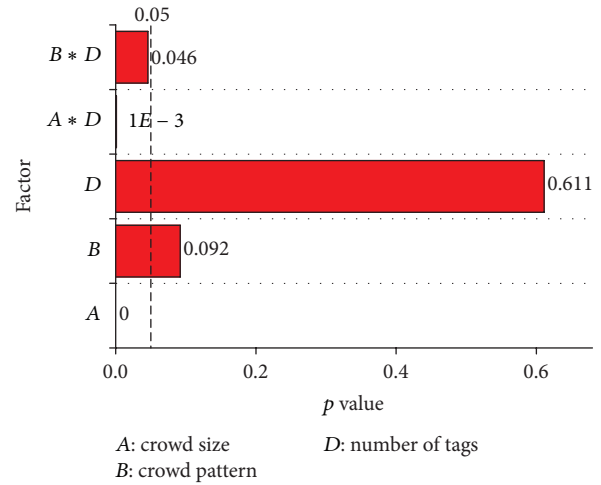


FIGURE 8: Second iteration of ANOVA for the RSSI (average) using adjusted sum of squares for tests.

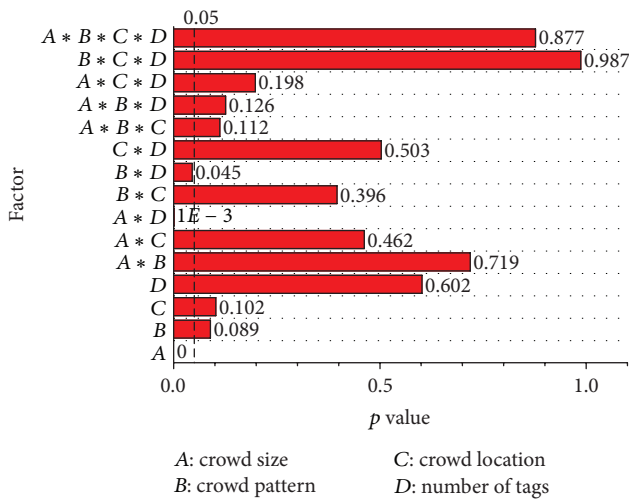


FIGURE 7: The  $p$  value from the analysis of variance for RSSI (average) using adjusted sum of squares for tests.

Figure 9(a) indicates that as the number of the tags increases to two and three, the RSSI values become smaller provided that the crowd size is between 10 and 15 people. Figure 9(b) shows that, on average, a lumped human crowd pattern inflicts 2.57 dBm more signal loss than the scattered pattern. The difference between them is denoted by  $X_{IE}$ . Figure 9(b) also illustrates that there is an improvement in the RSSI measurement if three tags are used in lumped human crowd pattern. This is possible as higher number of people in a crowd may create different crowd patterns and therefore gaps between one person and the other with respect to the tags.

As a summary, the strongest factor affecting the signal propagation is the human crowd size while two of

the strongest interactions are the combinations of human crowd size and crowd pattern with the number of tags. Using higher number of tags allows enhancement in the RSSI measurement due to the variation of the human crowd obstructions.

**3.3. Human Crowd Density Estimation Classifications.** The DOE data fitted into the H-CDE algorithm is shown in Figure 10. The classification has yielded 75.00% and 70.83% estimation accuracy for LD and MD, respectively. MD has lower estimation accuracy as a number of predictions were wrongly classified as LD, which can be attributed to the irregular gaps between the bodily obstructions, allowing the T-R signal to propagate better.

From (2), the signal path loss propagation model is fitted as

$$PL = PL_0 - 10n \log_{10}(d) - X_{IE} - 0.84m, \quad (3)$$

where  $PL_0$  is  $-32$  dBm,  $n$  measured at 35 m of line-of-sight of the T-R separation is 1.02,  $X_{IE}$  is 2.57 dBm, and multiplying  $m$ , the number of people, with 0.84 is the average body attenuation factor measured from three tags placements. The comparison between the models with the empirical data is imaged in Figure 11. As the distribution of data is quite diverse, the model is usable to predict the average RSSI of each crowd size. The model allows a quick human density prediction if the number of people can be estimated, which may be helpful in simulation software.

The empirical model has two assumptions to address its limitations. First, the model assumes that the highest signal loss is at the torso region [27, 28]. Secondly, it is assumed that the most dominant transmitted signal would be from the direct rays reflected, refracted, and diffused from the human body.

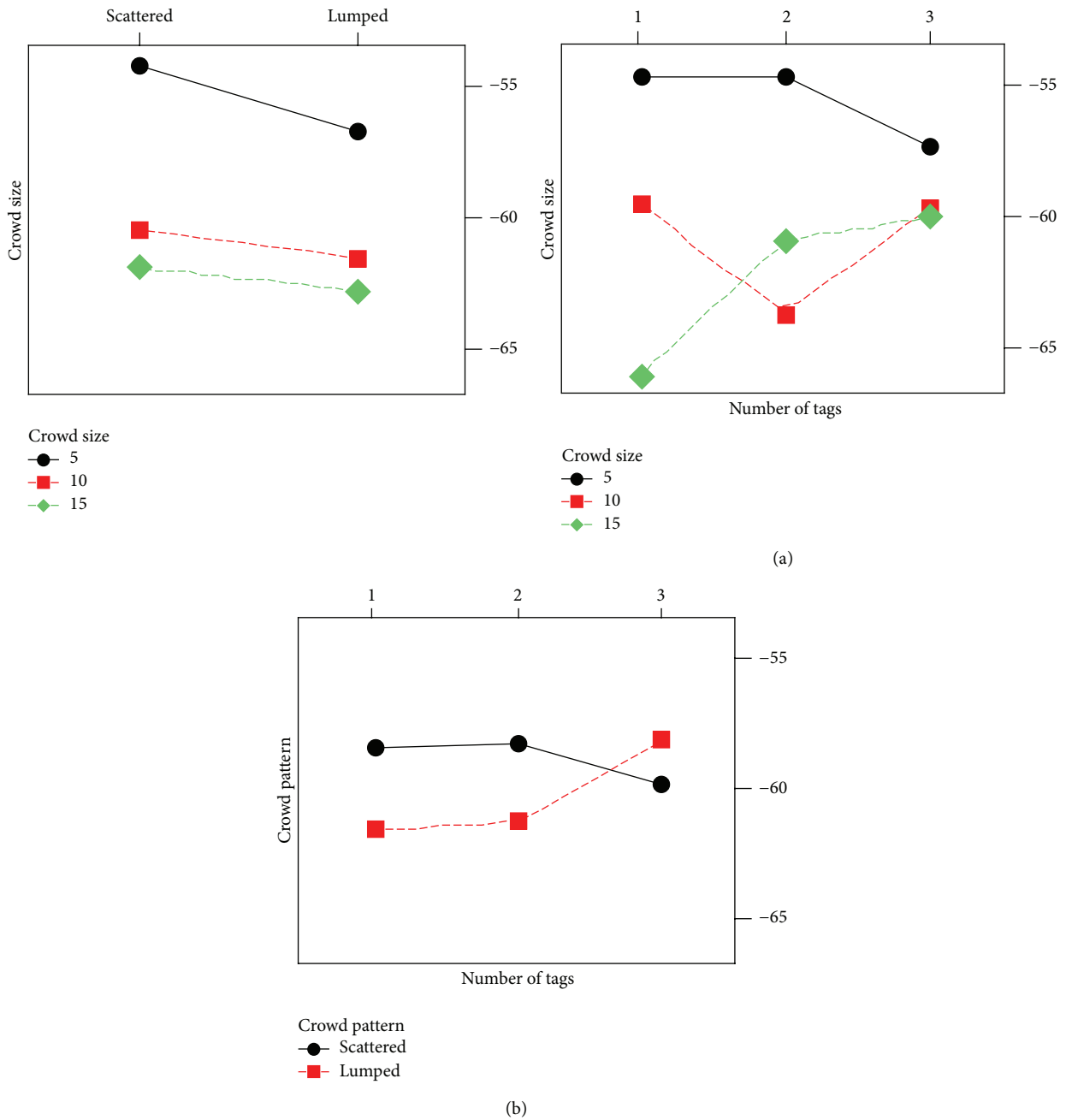


FIGURE 9: Interaction plot for the RSSI in dBm. (a) A combination of the human crowd size and number of tags and (b) a combination of the human crowd pattern with number of tags.

#### 4. Conclusion

The One-Way ANOVA test has proven that the dynamic and static crowds statistically incur the same mean of the signal attenuation. The DOE test has identified the human crowd size as the main factor influencing the signal attenuation in the human crowds. It also has recognized two significant interaction effects which are the number of tags in combination with the human crowd size and crowd pattern.

The findings of the DOE test used to train the H-CDE system enable the classification of the human crowd density into low, mediocre, or high category. The results of the DOE test fitted into the signal path loss propagation model ease the prediction of the human crowd density and potential simulation. Therefore, the human crowd properties which are verified by using the statistical approach are capable of creating a new approach in understanding and estimating the human crowd density especially for safety monitoring purposes.

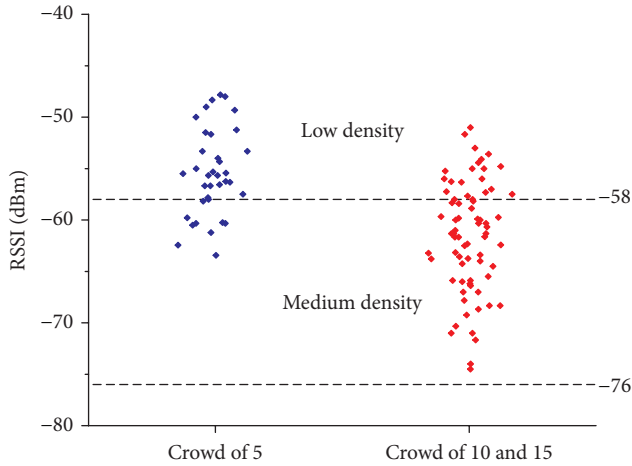


FIGURE 10: Classifying the density of the experimental data where each rhombus represents the average of 10 RSSI measurements.

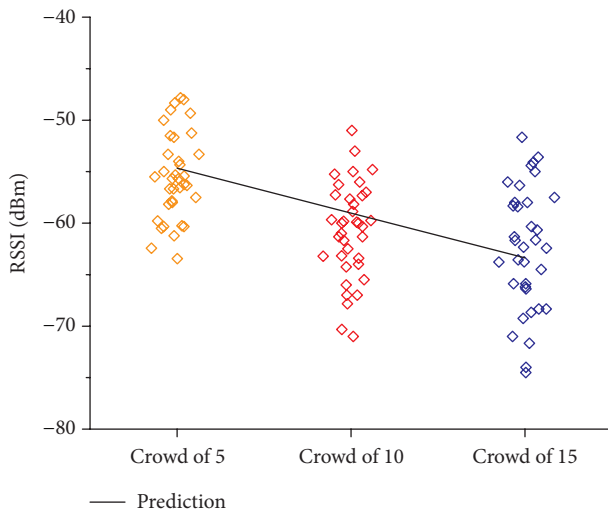


FIGURE 11: Comparison between the prediction model with the RSSI of different crowd size. Each rhombus represents the average of 10 RSSI measurements.

## Conflict of Interests

The authors declare that there is no conflict of interests regarding the publication of this paper.

## Acknowledgments

The authors would like to thank the funding sources for this work, which are Universiti Sains Malaysia and Malaysia Ministry of Higher Education Grant Secretariat for sponsoring the research under FRGS Grant 6071306.

## References

- [1] L. M. P. L. de Brito and L. M. R. Peralta, "An analysis of localization problems and solutions in wireless sensor networks," *Polytechnical Studies Review*, vol. 6, pp. 1–27, 2008.
- [2] A. Boukerche, H. A. B. F. Oliveira, E. F. Nakamura, and A. A. F. Loureiro, "Localization systems for wireless sensor networks," *IEEE Wireless Communications*, vol. 14, no. 6, pp. 6–12, 2007.
- [3] L. M. Ni, Y. Liu, Y. C. Lau, and A. P. Patil, "LANDMARC: indoor location sensing using active RFID," in *Proceedings of the 1st IEEE International Conference on Pervasive Computing and Communications (PerCom '03)*, pp. 407–415, IEEE, Fort Worth, Tex, USA, March 2003.
- [4] C.-N. Huang and C.-T. Chan, "ZigBee-based indoor location system by k-nearest neighbor algorithm with weighted RSSI," *Procedia Computer Science*, vol. 5, pp. 58–65, 2011.
- [5] A. Oka and L. Lampe, "Distributed target tracking using signal strength measurements by a wireless sensor network," *IEEE Journal on Selected Areas in Communications*, vol. 28, no. 7, pp. 1006–1015, 2010.
- [6] P. Bahl and V. N. Padmanabhan, "RADAR: an in-building RF-based user location and tracking system," in *Proceedings of the 19th Annual Joint Conference of the IEEE Computer and Communications Societies (INFOCOM '00)*, vol. 2, pp. 775–784, IEEE, Tel Aviv, Israel, March 2000.
- [7] Z. Dian and L. M. Ni, "Dynamic clustering for tracking multiple transceiver-free objects," in *Proceedings of the IEEE International Conference on Pervasive Computing and Communications (PerCom '09)*, pp. 1–8, Galveston, Tex, USA, March 2009.
- [8] C. Xu, B. Firner, R. S. Moore et al., "SCPL: indoor device-free multi-subject counting and localization using radio signal strength," in *Proceedings of the 12th International Conference on Information Processing in Sensor Networks (IPSN '13)*, pp. 79–90, Philadelphia, Pa, USA, April 2013.
- [9] CNN Network, "717 people dead: what caused the Hajj stampede?" October 2015, <http://edition.cnn.com/2015/09/25/middleeast/hajj-pilgrimage-stampede/index.html>.
- [10] Y. Mowafi, A. Zmily, D. E. D. I. Abou-Tair, and D. Abu-Saymeh, "Tracking human mobility at mass gathering events using WISP" in *Proceedings of the 2nd International Conference on Future Generation Communication Technologies (FGCT '13)*, pp. 157–162, IEEE, London, UK, November 2013.
- [11] J. Weppner, P. Lukowicz, U. Blanke, and G. Troster, "Participatory bluetooth scans serving as urban crowd probes," *IEEE Sensors Journal*, vol. 14, no. 12, pp. 4196–4206, 2014.
- [12] A. Morrison, M. Bell, and M. Chalmers, "Visualisation of spectator activity at stadium events," in *Proceedings of the 13th International Conference on Information Visualisation (IV '09)*, pp. 219–226, Barcelona, Spain, July 2009.
- [13] Y. Yuan, "Crowd monitoring using mobile phones," in *Proceedings of the 6th International Conference on Intelligent Human-Machine Systems and Cybernetics (IHMSC '14)*, vol. 1, pp. 261–264, IEEE, Hangzhou, China, August 2014.
- [14] J. Weppner and P. Lukowicz, "Bluetooth based collaborative crowd density estimation with mobile phones," in *Proceedings of the 11th IEEE International Conference on Pervasive Computing and Communications (PerCom '13)*, pp. 193–200, San Diego, Calif, USA, March 2013.
- [15] W. Xi, J. Zhao, X.-Y. Li et al., "Electronic frog eye: counting crowd using WiFi," in *Proceedings of the 33rd Annual IEEE International Conference on Computer Communications (INFOCOM '14)*, pp. 361–369, IEEE, Toronto, Canada, April-May 2014.
- [16] Y. Yuan, J. Z. Zhao, C. Qiu, and W. Xi, "Estimating crowd density in an RF-based dynamic environment," *IEEE Sensors Journal*, vol. 13, no. 10, pp. 3837–3845, 2013.
- [17] L. Haochao, E. C. L. Chan, G. Xiaonan, X. Jiang, W. Kaishun, and L. M. Ni, "Wi-counter: smartphone-based people counter

- using crowdsourced wi-fi signal data,” *IEEE Transactions on Human-Machine Systems*, vol. 45, no. 4, pp. 442–452, 2015.
- [18] M. Arai, H. Kawamura, and K. Suzuki, “Estimation of ZigBee’s RSSI fluctuated by crowd behavior in indoor space,” in *Proceedings of the SICE Annual Conference (SICE ’10)*, pp. 696–701, Taipei, Taiwan, August 2010.
- [19] G. K. Still, *Crowd dynamics [Ph.D. thesis]*, University of Warwick, 2000.
- [20] I. Karamouzas, B. Skinner, and S. J. Guy, “Universal power law governing pedestrian interactions,” *Physical Review Letters*, vol. 113, no. 23, Article ID 238701, 2014.
- [21] O. Litvinski and A. Gherbi, “Openstack scheduler evaluation using design of experiment approach,” in *Proceedings of the 16th IEEE International Symposium on Object/Component/Service-Oriented Real-Time Distributed Computing (ISORC ’13)*, pp. 1–7, Paderborn, Germany, June 2013.
- [22] X.-L. Liu, Y.-G. Chen, X.-R. Jing, and Y.-W. Chen, “Design of experiment method for microsatellite system simulation and optimization,” in *Proceedings of the International Conference on Computational and Information Sciences (ICIS ’10)*, pp. 1200–1203, IEEE, Chengdu, China, December 2010.
- [23] S. Y. Fadhlullah and W. Ismail, “Solar energy harvesting design framework for 3.3 V small and low-powered devices in wireless sensor network,” in *Proceedings of the 1st International Conference on Telematics and Future Generation Networks*, pp. 89–94, IEEE, Kuala Lumpur, Malaysia, May 2015.
- [24] S. Curtis, S. J. Guy, B. Zafar, and D. Manocha, “Virtual Tawaf: a case study in simulating the behavior of dense, heterogeneous crowds,” in *Proceedings of the IEEE International Conference on Computer Vision Workshops (ICCV ’11)*, pp. 128–135, IEEE, Barcelona, Spain, November 2011.
- [25] N. A. Shuaibu, I. Faye, M. T. Simsim, and A. S. Malik, “Spiral path simulation of pedestrian flow during Tawaf,” in *Proceedings of the 3rd IEEE International Conference on Signal and Image Processing Applications (ICSIPA ’13)*, pp. 241–245, Melaka, Malaysian, October 2013.
- [26] L. Azpilicueta, P. López-Iturri, E. Aguirre et al., “Analysis of radio wave propagation for ISM 2.4 GHz wireless sensor networks in inhomogeneous vegetation environments,” *Sensors*, vol. 14, no. 12, pp. 23650–23672, 2014.
- [27] E. Aguirre, J. Arpon, L. Azpilicueta, S. De Migue, V. Ramos, and F. J. Falcone, “Evaluation of electromagnetic dosimetry of wireless systems in complex indoor scenarios with human body interaction,” *Progress in Electromagnetics Research B*, vol. 43, pp. 189–209, 2012.
- [28] E. Reusens, W. Joseph, B. Latré et al., “Characterization of on-body communication channel and energy efficient topology design for wireless body area networks,” *IEEE Transactions on Information Technology in Biomedicine*, vol. 13, no. 6, pp. 933–945, 2009.